ISSN 1063-7788, Physics of Atomic Nuclei, 2016, Vol. 79, No. 6, pp. 835–841. © Pleiades Publishing, Ltd., 2016.

NUCLEI
Theory

Random Matrix Analysis of the Monopole Strength Distribution in ^{208}Pb*

A. P. Severyukhin[1),2)**], S. Åberg[3)], N. N. Arsenyev[1)], R. G. Nazmitdinov[4),1),2)], and K. N. Pichugin[5)]

Received April 8, 2016

Abstract—We study statistical properties of the 0^+ spectrum of ^{208}Pb in the energy region $E_x \leq 20$ MeV. We use the Skyrme interaction SLy4 as our model Hamiltonian to create a single-particle spectrum and to analyze excited states. The finite-rank separable approximation for the particle–hole interaction enables us to perform the calculations in large configuration spaces. We show that while the position of the monopole resonance centroid is determined by one-phonon excitations of 0^+, the phonon–phonon coupling is crucial for the description of the strength distribution of the 0^+ spectrum. In fact, this coupling has an impact on the spectral rigidity $\Delta_3(L)$ which is shifted towards the random matrix limit of the Gaussian orthogonal ensembles.

DOI: 10.1134/S1063778816060223

1. INTRODUCTION

Nuclear Giant Resonances (GR) are the subject of numerous investigations over several decades [1]. Some of the basic features such as centroids and collectivity (in terms of the sum rules) are reasonably well understood within microscopic theories [2–4]. As yet we have no answer to the question how a collective mode like the GR dissipates its energy.

According to the accepted wisdom, GRs are essentially excited by an external field through a one-body interaction. It is, therefore, natural to describe these states as collective 1p–1h states. Once excited, the GR progresses to a fully equilibrated system via direct particle emission and by coupling to more complicated configurations (2p–2h, 3p–3h, etc.). The former mechanism gives rise to an escape width. It is expected that the decay evolution along the hierarchy of more complex configurations till compound states determines spreading widths. A full description of this decay represents a fundamental problem which is, however, difficult to solve (if even is possible at all?) due to existence of many degrees of freedom for many-body quantum system such as a nucleus. Therefore, to gain an insight into the nature of GR spreading we have to introduce various approximations or a model, which validity depends on a primal feasibility.

In general, the description of GR properties is based on the analysis of the electromagnetic strength distribution in an energy interval which is large enough to catch hold of basic GR features that is under investigation. An obvious requirement to the model consideration is to use configurations with various degrees of complexity. Evidently, the more complex configuration is considered, the more cumbersome task should be solved. Therefore, a natural question arises: what type of a particular complex configuration should be enough in order to understand the gross structure of a particular GR which data are available in modern experiments? In addition, once this complex configuration is defined one can further ask about statistical properties of states that compose the GR strength distribution. As a result, one could illuminate the role of various correlations that diminish the importance of a specific excitation that determines the centroid position of a specific GR.

To answer these questions we will employ two approaches. On the one hand, the random matrix theory (RMT) [5–9] provides necessary tools to shed light on the spectral properties and the distribution of transition-strength properties, when specific features become not of a primary importance. The RMT assumes only that the nuclear Hamiltonian belongs to an ensemble of random matrices that are consistent with the fundamental symmetries of the system. In particular, in the case of the time-reversal symmetry,

*The text was submitted by the authors in English.

1)Bogoliubov Laboratory of Theoretical Physics, Joint Institute for Nuclear Research, Dubna, Russia.
2)Dubna State University, Russia.
3)Mathematical Physics, LTH, Lund University, Sweden.
4)Departament de Física, Universitat de les Illes Balears, Spain.
5)Kirensky Institute of Physics, Krasnoyarsk, Russia.
**E-mail: sever@theor.jinr.ru

the relevant ensemble is the Gaussian orthogonal ensemble (GOE). On the other hand, to understand the fragmentation of high-lying states it is necessary also to exploit nuclear structure models that are based on the microscopic many-body theory, where the effects of the residual interaction on the statistics must be studied in large model spaces. Introducing a residual interaction in general implies a transition to GOE properties above some excitation energy [10].

The quasiparticle–phonon model (QPM) [4] offers an attractive framework for such studies. The separable form of the residual interaction of a model Hamiltonian allows to diagonalize it in a space spanned by states composed of one, two, and three phonons considered in the random-phase approximation (RPA). We would like to mention here the RMT analysis of statistical properties of a pygmy dipole resonance within the QPM, based on the Woods–Saxon potential [11]. It is desirable, however, to use a unified approach in which a mean field and a residual interaction are treated on the same footing in order to avoid any artifacts [12, 13]. For our purposes we choose the modern development of the QPM, the finite rank separable approximation (FRSA) [14–16]. The FRSA follows the basic QPM ideas, but the single-particle (sp) spectrum and the residual interaction are calculated with the Skyrme forces. This approach enables us to consider a coupling between the one- and two-phonon components of the wave functions [17]. It was successfully used to study the properties of the low-lying states and giant resonances within the RPA and beyond [14–19].

By means of this approach and by the RMT tools we attempt in this paper to understand the complex structure observed in the 0^+ spectrum of the doubly-magic nucleus ^{208}Pb in the region of the isoscalar giant monopole resonance (ISGMR). This strength distribution is extensively studied in many experiments [20–23]. The experimental properties have been described within the RPA with the Skyrme interactions (for a review see, for example, [24]). In this system the effect of the anharmonicity is expected to be small. Contrary to the expectations, we will show the importance of the phonon–phonon coupling (PPC) effects for the statistical properties of the spectrum calculated with the aid of the Skyrme SLy4 interaction, taken as an example.

2. THE MODEL

For the analysis of the doubly magic nucleus we impose a spherical symmetry on the sp wave functions in our HF calculations. The continuous part of the sp spectrum is discretized by diagonalizing the HF Hamiltonian on a harmonic oscillator basis. The cut-off of the continuous part is at the energy of 100 MeV. As the parameter set, we use the Skyrme force SLy4 [25] which was adjusted to reproduce the nuclear matter properties, as well as nuclear charge radii, binding energies of doubly-magic nuclei. The residual particle–hole interaction is obtained as the second derivative of the energy density functional with respect to the particle density. By means of the standard procedure [26] we obtain the familiar RPA equations in the 1p–1h configuration space. The eigenvalues of the RPA equations are found numerically as the roots of a relatively simple secular equation within the FRSA [14]. Since the FRSA enables to us to use the large 1p–1h space, there is no need in effective charges.

Using the basic QPM ideas in the simplest case of the configuration mixing [4], we construct the wave functions from a linear combination of one- and two-phonon configurations states as

$$\Psi_\nu(JM) = \Bigg\{\sum_i R_i(J\nu)Q^+_{JMi} + \sum_{\lambda_1 i_1 \lambda_2 i_2} P^{\lambda_1 i_1}_{\lambda_2 i_2}(J\nu)\left[Q^+_{\lambda_1\mu_1 i_1} Q^+_{\lambda_2\mu_2 i_2}\right]_{JM}\Bigg\}|0\rangle, \quad (1)$$

where $Q^+_{\lambda\mu i}|0\rangle$ is the RPA excitation having energy $\omega_{\lambda i}$; λ denotes the total angular momentum, and μ is its z projection in the laboratory system. The ground state is the RPA phonon vacuum $|0\rangle$. The normalization condition for the wave functions (1) yields

$$\sum_i R_i^2(J\nu) + 2\sum_{\lambda_1 i_1 \lambda_2 i_2} (P^{\lambda_1 i_1}_{\lambda_2 i_2}(J\nu))^2 = 1. \quad (2)$$

The variational principle leads to a set of linear equations for unknown amplitudes $R_i(J\nu)$ and $P^{\lambda_1 i_1}_{\lambda_2 i_2}(J\nu)$ [17]:

$$(\omega_{Ji} - E_\nu)R_i(J\nu) + \sum_{\lambda_1 i_1 \lambda_2 i_2} U^{\lambda_1 i_1}_{\lambda_2 i_2}(Ji)P^{\lambda_1 i_1}_{\lambda_2 i_2}(J\nu) = 0, \quad (3)$$

$$\sum_i U^{\lambda_1 i_1}_{\lambda_2 i_2}(Ji)R_i(J\nu) + 2(\omega_{\lambda_1 i_1} + \omega_{\lambda_2 i_2} - E_\nu)P^{\lambda_1 i_1}_{\lambda_2 i_2}(J\nu) = 0. \quad (4)$$

The rank of the set of linear equations is equal to the number of one- and two-phonon configurations included in the wave function (1). To resolve this set it is required to compute the coupling matrix elements

$$U^{\lambda_1 i_1}_{\lambda_2 i_2}(Ji) = \langle 0|Q_{Ji}H\left[Q^+_{\lambda_1 i_1}Q^+_{\lambda_2 i_2}\right]_J|0\rangle \quad (5)$$

between one- and two-phonon configurations (see details in [17]). Evidently, the nonzero matrix elements $U^{\lambda_1 i_1}_{\lambda_2 i_2}(Ji)$ result in the inclusion of the PPC effects. Equations (3) and (4) have the same form as the QPM equations [4]. It is important to stress, however, that the sp spectrum and the parameters of the residual p–h interaction are calculated with the chosen Skyrme forces, without any further adjustments.

The excitation operator of the ISGMR is defined as

$$\hat{M}_{L=0} = \sum_{i=1}^{A} r_i^2. \quad (6)$$

The wave functions (1) allow us to determine the transition probabilities $\left|\langle 0^+_\nu|\hat{M}_{L=0}|0^+_{\rm g.s}\rangle\right|^2$. The matrix elements for direct excitation of two-phonon components from the ground state are about two orders of magnitude smaller as compared to the excitation of one-phonon components [4]. Therefore, they are neglected in our calculation of the transition probabilities. The RPA analysis of the ISGMR shows that 96% of the non-energy-weighted sum rules (NEWSR) are located in the energy region $E_x = 10.5–18$ MeV. To build the wave functions (1) of the excited 0^+ states up to 20 MeV we take into account all one- and two-phonon configurations $[\lambda^\pi_{i_1} \otimes \lambda^\pi_{i_2}]_{\rm RPA}$ that are constructed from the 0^+, 1^-, 2^+, 3^-, and 4^+ phonons with energies below 25 MeV for computational convenience. The high-energy configurations plays a minor role in our calculations. It is noteworthy that the pair-transfer mode (see, e.g., [27, 28]) is outside the present work.

Properties of the low-energy two-phonon 0^+ states are reflected in the deviation from the harmonic picture for the multiphonon excitations [29, 30]. It is interesting to study the energies, and reduced transition probabilities of the $[2^+_1]_{\rm RPA}$, $[3^-_1]_{\rm RPA}$, and $[4^+_1]_{\rm RPA}$ states which are the important ingredients of our calculations of the two-phonon 0^+ states of ^{208}Pb. The results obtained within the one-phonon approximation are compared with the experimental data [31, 32] in the table. There is a satisfactory description of the reduced transition probabilities. The overestimate of the experimental energies indicates some missing mechanisms. In our consideration we consider the PPC as the one that might improve the description.

The strength distribution of ISGMR is displayed in Fig. 1. Both experimental [22] and theoretical results show the fragmentation and splitting of the ISGMR strength. The coupling between the one- and two-phonon states yields a noticeable redistribution of the ISGMR strength in comparision with the RPA results. In particular, the coupling decreases the NEWSR till 78% in the ISGMR region ($E_x = 10.5–18$ MeV). Also, the PPC induces the 1-MeV downward shift of the main peak. There are the low-energy part, the main peak and the high-energy tail. The coupling produces a shift of order 11% (7%) of the NEWSR from the ISGMR region to the high (lower) energy region. The strength distribution of the ISGMR obtained within the PPC is rather close to the experimental distribution [22]. Our analysis shows that the major contribution to the strength distribution is brought about by the coupling between the $[0^+]_{\rm RPA}$ and $[3^- \otimes 3^-]_{\rm RPA}$ components. We recall that the importance of the complex configurations for the interpretation of basic peculiarities of the ISGMR strength distribution of ^{208}Pb was already qualitatively discussed in the framework of a simple model [33, 34]. Our calculations give the same tendency.

Energy and $B(E\lambda)$ values for up-transitions to the λ^π_1 states in ^{208}Pb (Experimental data are taken from [31, 32])

λ^π_1	Energy, MeV		$B(E\lambda; 0^+_{\rm g.s} \to \lambda^\pi_1)$, e^2 b$^\lambda$	
	Exp.	RPA	Exp.	RPA
3^-_1	2.62	3.6	0.611 ± 0.012	0.93
2^+_1	4.09	5.2	0.318 ± 0.016	0.34
4^+_1	4.32	5.6	0.155 ± 0.011	0.15

We turn now to the mechanism that dominates in the low-energy part of the 0^+ spectrum. There is no $[0^+]_{\rm RPA}$ state below 10.2 MeV. The extension of the variational space from the standard RPA to two-phonon configurations result in a formation of the low-lying 0^+ states. The $[3^-_1]_{\rm RPA}$ state is the lowest excitation which leads to the minimal two-phonon energies and the maximal matrix elements coupling between one- and two-phonon configurations. Since the PPC induces a downward shift of the 0^+_1 energy, the energy state at 6.5 MeV is very close to the value $\sim 2\hbar\Omega$ with $\hbar\Omega = E^{RPA}_{3^-_1}$ (see table). Our analysis suggests the dominance ($\geq$85%) of the octupole $[3^-_1 \otimes 3^-_1]_{\rm RPA}$, $[3^-_1 \otimes 3^-_2]_{\rm RPA}$, and $[3^-_1 \otimes 3^-_3]_{\rm RPA}$ configurations in the wave functions of the excited 0^+_1, 0^+_2, and 0^+_3 states, respectively. The collective character of the 0^+_1 state is mainly due to their coupling to the ISGMR, produced by the $[0^+_4]_{\rm RPA}$ state. In particular, the wave function normalization of the 0^+_1 state contains 4% of the $[0^+_4]_{\rm RPA}$. This small change in

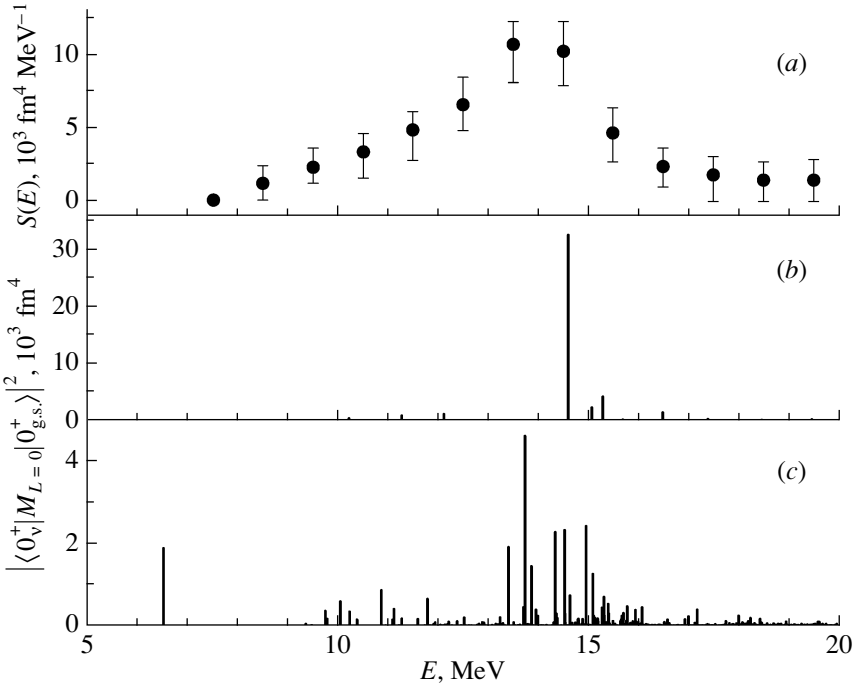

Fig. 1. The PPC effect on the isoscalar monopole strength distribution in ^{208}Pb. Panel (a): experimental strength distribution is taken from [22]. Panels (b) and (c) correspond to the calculations within the RPA and taking into account the PPC, respectively.

structure has a large impact on the $\left|\langle 0^+_1|\hat{M}_{L=0}|0^+_{\rm g.s}\rangle\right|^2$ value, see Fig.1. The lowest two-phonon 0^+ state was first observed as the lowest-spin member of the $[3^-_1 \otimes 3^-_1]$ multiplet in [35]. This fact was confirmed by the QPM analysis [30].

3. SPECTRAL STATISTICS

Let us study statistical properties of the 0^+ spectrum up to 20 MeV. We examine the spectra calculated with and without the PPC effects, i.e., the cases of $U \neq 0$ and $U = 0$, respectively. Figure 2 displays the PPC impact on the 0^+ energies. As was mentioned above, the coupling shifts down the part of 0^+ states and modifies the level density. To elucidate the role of the residual interaction we also consider the 0^+ spectrum of unperturbed 1p–1h and 2p–2h states (see Fig. 2a). Note that the level density of the unperturbed 3p–3h states is much smaller than the 2p–2h ones. As can be seen from Fig. 2, the difference between the unperturbed p–h and the $U = 0$ spectra is remarkable. The downward shift of the $U = 0$ spectrum is due to the residual interaction in the RPA framework. The coupling does not lead to visible spectrum changes. However, it brings important correlations that affect the spectral statistics.

The three spectra are analyzed within the RMT that enables us to study the statistical laws governing fluctuations that, in general, can have very different origins. Starting from the spectrum E_i, one can construct the staircase function $N(E)$ which is defined as the state number below the energy E. The function $N(E)$ can be separated in a smooth part $S(E)$ and the fluctuating part $N_{\rm fluct}(E)$, where the integral of $N_{\rm fluct}(E)$ is zero. The function $S(E)$ can be determined either from semiclassical arguments or using a polynomial for $N(E)$. To get a constant mean spacing of levels, we employ the unfolded spectrum defined by the mapping $x_i = S(E_i)$. Note that the values $s_i = x_{i+1} - x_i$ are introduced as the spacings. We use two typical measures to analyze the fluctuation properties of unfolded spectrum: the nearest-neighbor spacing distribution (NNSD) and the spectral rigidity of Dyson and Metha, the Δ_3 statistics [36].

Due to the unfolding we have

$$\int_0^\infty sP(s)ds = 1. \tag{7}$$

If the unfolded energies x_i are in a regular system then the NNSD is known as the Poisson distribution,

$$P(s) = e^{-s}. \tag{8}$$

In the GOE, i.e. the energies are in a chaotic system, the NNSD is approximately given as the Wigner distribution [6],

$$P(s) = (\pi/2)s\exp(-\pi s^2/4). \tag{9}$$

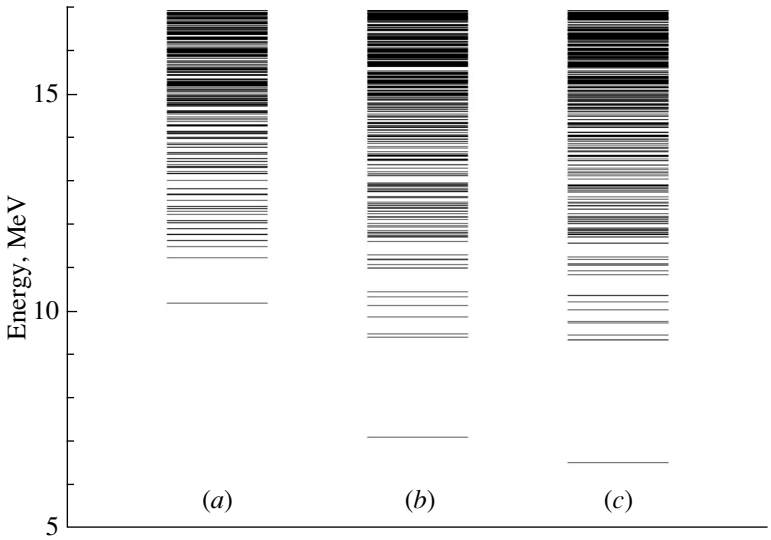

Fig. 2. Calculated spectra of the 0^+ states of ^{208}Pb. The unperturbed 1p–1h and 2p–2h energies are shown in column (a). Columns (b) and (c) correspond to the calculations without and with the effects of the PPC, respectively.

As can be seen from Fig. 3, for the unperturbed p–h spectrum we obtain a behavior close to the Poisson distribution, expected for uncorrelated energies. For the case of $U \neq 0$, the statistics is changing to the GOE limit. This fact indicates the onset of correlations that redistribute a $[0^+]_{\mathrm{RPA}}$ strength over two-phonon components constructed by phonons with the other multipolarities. Indeed, the comparison of the NNSD without and with the coupling illuminates this fact evidently. At $U = 0$ the spectrum is characterized by the Poisson (uncorrelated) statistics. The coupling between the one- and two-phonon components modifies the spectrum, and the NNSD becomes close to the Wigner surmise.

Another measure of correlations is the Δ_3 statistics defined as

$$\Delta_3(\alpha, L) = \min_{A,B} \frac{1}{L} \int_{\alpha}^{\alpha+L} \left[N(x) - (Ax + B)\right]^2 dx. \quad (10)$$

It characterizes the deviation of the staircase function $N(x)$ from a straight line, and the rigid unfolded spectrum corresponds to smaller values of Δ_3, while the soft spectrum has a larger Δ_3. In fact, for a given L, smaller values of Δ_3 imply stronger long-range correlations between the levels.

For the sake of convenience, the function $\Delta_3(\alpha, L)$, averaged over n_α intervals $(\alpha, \alpha + L)$

$$\bar{\Delta}_3(L) = \frac{1}{n_\alpha} \sum_{\alpha} \Delta_3(\alpha, L), \quad (11)$$

can be easily calculated from the number statistics, $n(L)$, which is the number of levels in an energy interval of length L

$$\bar{\Delta}_3(L) = \frac{2}{L^4} \int_0^L \left(L^3 - 2L^2 r + r^3\right) \Sigma^2(r) dr, \quad (12)$$

$$\Sigma^2(L) = \left\langle [n(L) - \langle n(L) \rangle]^2 \right\rangle. \quad (13)$$

For an uncorrelated spectrum one has

$$\bar{\Delta}_3(L) = L/15, \quad (14)$$

while for the GOE it is

$$\bar{\Delta}_3(L) \approx \frac{1}{\pi^2}(\ln L - 0.0687) \quad (15)$$

in the $L \gg 1$ limit. Figure 4 demonstrates the evolution of the Δ_3 measure from the uncorrelated states to the GOE limit, when the PPC effects are only responsible for the statistical correlations. These correlations dissolve the collective ISGMR in the sea of the fragmented two-phonon 0^+ components created by the other multipolarities.

4. SUMMARY

With the aid of a finite rank separable approximation we have analyzed the strength distribution of 0^+ states ($E_x \leq 20$ MeV) of ^{208}Pb. To simulate the mean field we have used the SLy4 Skyrme interaction. To analyze the 0^+ excitations we take into account all RPA states with $\lambda^\pi = 0^+, 1^-, 2^+, 3^-, 4^+$. Within the RPA approach the centroid location of the ISGMR is found at $E \sim 14.7$ MeV. On the other hand, we have

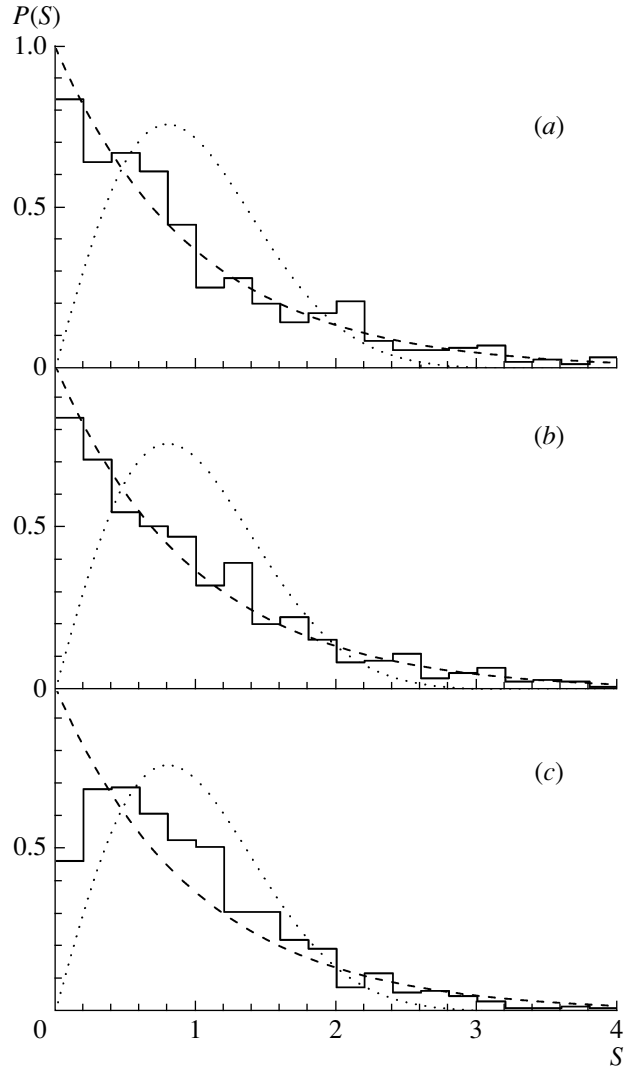

Fig. 3. The nearest-neighbor spacing distribution for calculated spectra of the 0^+ states of ^{208}Pb. The case of unperturbed 1p–1h and 2p–2h energies is shown in panel (a). Panels (b) and (c) correspond to the calculations without and with the PPC effects, respectively. The dotted line is the GOE limit and the dashed line is the Poisson statistics.

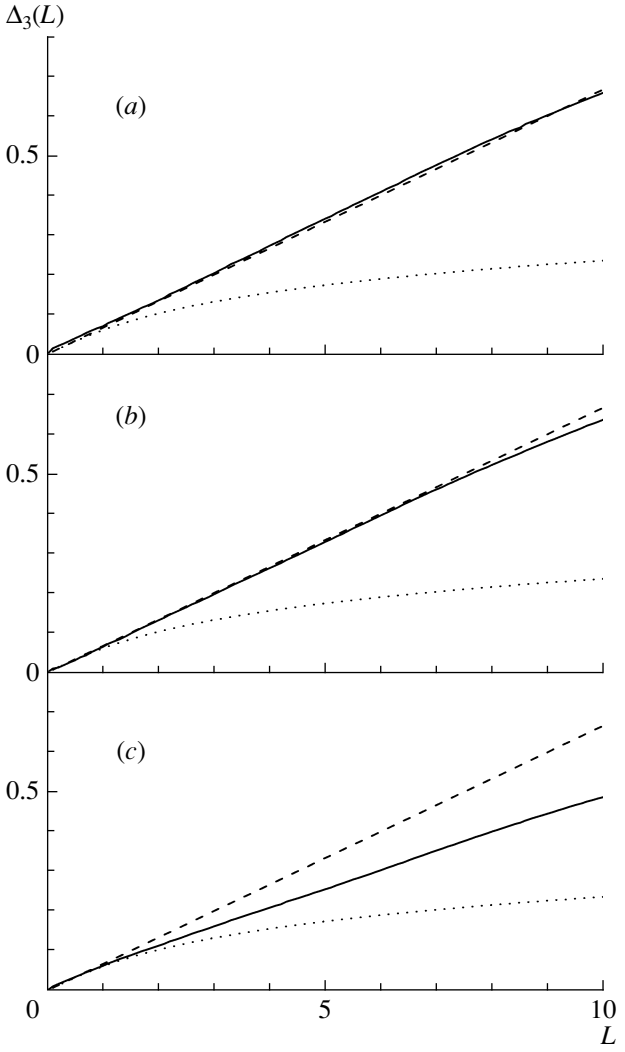

Fig. 4. The spectral rigidity $\Delta_3(L)$ for calculated spectra of the 0^+ states of ^{208}Pb. The case of unperturbed 1p–1h and 2p–2h energies is shown in panel (a). Panels (b) and (c) correspond to the calculations without and with the PPC effects, respectively. The dotted line is the GOE limit and the dashed line is the Poisson statistics.

demonstrated that the coupling between one- and two-phonon terms in the wave functions of excited states is crucially important for the interpretation of the strength distribution of the ISGMR in the energy interval $E_x \approx 10.5-18$ MeV. The results of the calculated transition-strength distribution are generally in a reasonable agreement with the experimental data.

The RMT measures such as the NNSD and the Δ_3 function indicate a transition towards GOE as soon as the coupling is switched on. It appears that the presence of two-phonon components in our wave function, in addition to the one-phonon ones, already enables us to describe the gross strength distribution of the ISGMR in the experimentally available energy interval. We observed that the major contribution that evolves the system under consideration to the GOE limit is brought about by two-pnonon components of the octupole nature. In fact, their number exceeds essentially the numbers of two-phonon components that are constructed from phonons with the other multipolarities. A further systematic statistical studies of the impact of the phonon–phonon coupling on the vibrational spectra and the $E\lambda$-transition strengths is clearly necessary and is in progress.

ACKNOWLEDGMENTS

A.P.S. thanks for the hospitality the Division of Mathematical Physics, Lund University, where a part

of this work has been done. This work was partly supported by Russian Foundation for Basic Research (project nos. 16-52-150003 and 16-02-00228).

REFERENCES

1. M. N. Harakeh and A. van der Woude, *Giant Resonances: Fundamental High-Frequency Modes of Nuclear Excitation* (Clarendon Press, Oxford, 2001).
2. A. Bohr and B. Mottelson, *Nuclear Structure, Vol. 2* (World Sci., Singapore, 1998).
3. A. B. Migdal, *Teoriya konechnykh fermi-sistem i svoistva atomnih yader*, 2nd ed. (Nauka, Moscow, 1983) [in Russian].
4. V. G. Soloviev, *Theory of Atomic Nuclei: Quasiparticles and Phonons* (Institute of Physics, Bristol; Philadelphia, 1992).
5. T. A. Brody, J. Flores, J. B. French, et al., Rev. Mod. Phys. **53**, 385 (1981).
6. M. L. Metha, *Random Matrices*, 2nd ed. (Academic, New York, 1991).
7. T. Guhr, A. Müller-Groeling, and H. A. Weidenmüller, Phys. Rept. **299**, 189 (1998).
8. H. A. Weidenmüller and G. E. Mitchell, Rev. Mod. Phys. **81**, 539 (2009).
9. J. M.G. Gómez, K. Kar, V. K. B. Kota, et al., Phys. Rept. **499**, 103 (2011).
10. S. Åberg, Phys. Rev. Lett. **64**, 3119 (1990).
11. J. Enders, T. Guhr, A. Heine, et al., Nucl. Phys. A **741**, 3 (2004).
12. E. E. Saperstein, S. A. Fayans, and V. A. Khodel, Fiz. Elem. Chastits At. Yadra **9**, 221 (1978) [Sov. J. Part. Nucl. **9**, 91 (1978)].
13. See discussion on self-consistent effects in various mesoscopic systems, for example, in J. L. Birman, R. G. Nazmitdinov, and V. I. Yukalov, Phys. Rept. **526**, 1 (2013).
14. Nguyen Van Giai, Ch. Stoyanov, and V. V. Voronov, Phys. Rev. C **57**, 1204 (1998).
15. A. P. Severyukhin, Ch. Stoyanov, V. V. Voronov, and Nguyen Van Giai, Phys. Rev. C **66**, 034304 (2002).
16. A. P. Severyukhin, V. V. Voronov, and Nguyen Van Giai, Phys. Rev. C **77**, 024322 (2008).
17. A. P. Severyukhin, V. V. Voronov, and Nguyen Van Giai, Eur. Phys. J. A**22**, 397 (2004).
18. A. P. Severyukhin, N. N. Arsenyev, and N. Pietralla, Phys. Rev. C **86**, 024311 (2012).
19. A. P. Severyukhin, N. N. Arsenyev, N. Pietralla, and V. Werner, Phys. Rev. C **90**, 011306(R) (2014).
20. D. H. Youngblood, H. L. Clark, and Y.-W. Lui, Phys. Rev. Lett. **82**, 691 (1999).
21. D. H. Youngblood, Y.-W. Lui, H. L. Clark, et al., Phys. Rev. C **69**, 034315 (2004).
22. D. Patel, U. Garg, M. Fujiwara, et al., Phys. Lett. B **726**, 178 (2013).
23. D. Patel, U. Garg, M. Itoh, et al., Phys. Lett. B **735**, 387 (2014).
24. N. Paar, D. Vretenar, E. Khan, and G. Colò, Rep. Prog. Phys. **70**, 691 (2007).
25. E. Chabanat, P. Bonche, P. Haensel, et al., Nucl. Phys. A **635**, 231 (1998).
26. J. Terasaki, J. Engel, M. Bender, et al., and M. Stoitsov, Phys. Rev. C **71**, 034310 (2005).
27. R. Julin, J. Kantele, J. Kumpulainen, et al., Phys. Rev. C **36**, 1129 (1987).
28. A. Heusler, T. Faestermann, R. Hertenberger, et al., Phys. Rev. C **91**, 044325 (2015).
29. E. G. Lanza, M. V. Andrés, F. Catara, et al., Nucl. Phys. A **613**, 445 (1997).
30. V. Yu. Ponomarev and P. von Neumann-Cosel, Phys. Rev. Lett. **82**, 501 (1999).
31. J. Heisenberg, J. Lichtenstadt, C. N. Papanicolas, and J. S. McCarthy, Phys. Rev. C **25**, 2292 (1982).
32. R. H. Spear, W. J. Vermeer, M. T. Esat, et al., Phys. Lett. B **128**, 29 (1983).
33. G. F. Bertsch, P. F. Bortignon, R. A. Broglia, and C. H. Dasso, Phys. Lett. B **80**, 161 (1979).
34. P. F. Bortignon and R. A. Broglia, Nucl. Phys. A **371**, 405 (1981).
35. M. Yeh, P. E. Garrett, C. A. McGrath, et al., Phys. Rev. Lett. **76**, 1208 (1996).
36. F. J. Dyson and M. L. Mehta, J. Math. Phys. **4**, 701 (1963).